A semi-distributed simulation model for natural pipeflow

J.A.A. Jones*, L.J. Connelly

Institute of Geography and Earth Sciences, University of Wales, Aberystwyth SY23 3DB, UK

Abstract

Field monitoring of natural pipeflow over the last two decades has demonstrated its potential importance both as a hillslope drainage process and as a source of streamflow, yet very few attempts have been made to model the process. The main model designed to simulate pipeflow to date is shown to be unrepresentative of the natural field situation. This paper describes a semi-distributed simulation model with physically based parameters that has been designed around the field situation, as monitored in the longest run field experiment on pipeflow. The results are encouraging, despite the fact that data on a number of relevant parameters can be difficult to obtain at less intensely studied field sites. © 2002 Elsevier Science B.V. All rights reserved.

Keywords: Soil pipes; Pipeflow modelling; Subsurface stormflow; Hillslope hydrology

1. Introduction

The importance of natural pipeflow in hillslope drainage and streamflow generation in source areas has been demonstrated by a number of field monitoring experiments in a variety of climatic regimes. This suggests that pipeflow processes need to be incorporated into general rainfall-runoff models. The present paper represents the first attempt to model the generation of pipeflow using a partially distributed, physically based simulation algorithm that has been constructed and tested on the basis of one of these field studies. It offers an initial step towards including pipeflow processes in catchment models.

1.1. Evidence for pipeflow contributions

There is now considerable evidence to suggest the importance of pipeflow to runoff generation in a wide range of environments. This evidence comes particu-

larly from Britain (Jones, 1978, 1981; Gilman and Newson, 1980; McCaig, 1983, 1984; Jones and Crane, 1984; Wilson and Smart, 1984; Jones, 1987, 1988; Jones et al., 1991; Sklash et al., 1996; Jones, 1997a,c,d; Holden and Burt, 2002), Japan (Yasuhara, 1980; Tanaka, 1982; Tsukamoto et al., 1982; Sidle et al., 1995; Terajima et al., 1996, 1997; Uchida et al., 1999; Terajima et al., 2000) and Canada, in the arid badlands of Alberta (Bryan and Harvey, 1985), the taiga (Roberge and Plamondon, 1987), and the tundra (Woo and diCenzo, 1988; Carey and Woo, 2000). Other evidence comes from the Loess Plateau of Shanxi, China (Zhu, 1997; Zhu et al., 2002), and in the Western Ghats in India (Putty and Prasad, 2000).

It is clear from these observations that pipeflow can be a very important contributor to streamflow in many headwater basins. It is also apparent that there are wide differences in the amount contributed in both space and time that are likely to complicate the search for general models.

The highest percentage contributions come from the Tama Hills near Tokyo, where Tsukamoto et al.

* Corresponding author.
  E-mail address: jaj@aber.ac.uk (J.A.A. Jones).

(1982) report that pipeflow contributes nearly 100% of water leaving a zero-order basin or hillside hollow and Yasuhara (1980) measured over 75% of ephemeral streamflow in a larger adjacent basin as deriving from pipes. Many estimates fall in the range 40–55% in mid-Wales (Jones, 1987) and in Honshu, Japan (Tanaka, 1982). Contributions of 20% and over have been reported in China, India and Canada. Zhu (1997) and Zhu et al. (2002) report contributions of 35% in the Loess Plateau along the Yellow River. In the Western Ghats, Southern India, monitoring by Putty and Prasad (2000) indicated an average of 25% of streamflow deriving from pipeflow. Measured contributions in Canada, range from 33% in Albertan badlands (Bryan and Harvey, 1985) down to 20–22% in snowmelt events in subarctic Yukon and southern Quebec (Carey and Woo, 2000; Roberge and Plamondon, 1987). Lower average contributions have been reported for deep-seated pipes in tropical soils and in deep blanket peats, and for some shallow ephemeral piping in Britain. On Dominica, Walsh and Howells (1988) estimated that only 16% of streamflow was derived from deep-seated pipeflow, although their survey did not cover the part of the island where shallow, more responsive soil piping is most likely to be found. Similarly, in a highly eroded British peat bog in northern England, Gardiner (1983) and Burt et al. (1990) estimated that only about 1% of streamflow was derived from pipeflow, but the study omitted to monitor flows from the larger pipes. More convincing evidence from a deep blanket peat catchment comes from Holden and Burt (2002) who monitored 10%, plus about 0.5% from hand-sampled pipes (Holden, personal communication). Woo and diCenzo (1988) also reported ephemeral pipes delivering just 10% of total runoff against 89% via overland flow in a subarctic wetland in northern Ontario. Similarly, Chapman (1994) and Chapman et al. (1997) report only a 10% contribution from shallow ephemeral pipes in the Centre for Ecology and Hydrology's Upper Wye experimental catchment in mid-Wales, adjacent to the Maesnant basin of Jones (1987). In this case, the difference is that the Maesnant basin contains larger perennially flowing pipes, and though these exist in parts of the Upper Wye, they have not been monitored and included as pipeflow. Interestingly, the direct contribution to streamflow from ephemeral pipes on Maesnant is very comparable, if the large proportion

of ephemeral pipeflow that feeds through the perennial pipes is excluded (v.i.).

A major problem for estimating contributions, and, indeed, for modelling pipeflow, is the high spatial variation in pipe discharges even over short distances and between adjacent pipes. Within the 23 ha of the Maesnant experiment, there is nearly an order of magnitude difference between perennial pipes in both mean stormflow discharge and peak discharges, and 60-fold differences between the smallest ephemeral and the largest perennial pipe (Jones, 1987).

There is also abundant evidence of wide differences between mean and peak contributions. Roberge and Plamondon (1987) reported peak contributions as high as 76% during snowmelt in Quebec. Putty and Prasad (2000) measured peaks of pipeflow contributions as high as 59% of total streamflow in their Indian basin. In the most favourable conditions on Maesnant, the percentage coming from pipes can reach 78%, but overland flow becomes relatively more important in the wettest conditions (Jones, 1987). Even in the deep peat bog, Holden and Burt (2002) note that on the rising and falling limbs pipeflow could account for over 30% of stream discharge, and that the dominant drainage process varies in time and space throughout storm response. Carey and Woo (2000) found 21% of runoff in their subarctic Yukon basin draining via pipes during the snowmelt period falling to under 3% during the summer rainfall period. Similarly, in the small 4 ha headwater catchment within the Upper Wye experimental catchment in Wales monitored by Chapman (1994) and Chapman et al. (1997), although average contributions from the ephemeral pipes only amounted to 10%, this rose to 32% in peak flow, or 38% in the table presented in Chapman et al. (1993). Further aspects of pipeflow are reviewed in Jones (1990, 1994, 1997b) and Bryan and Jones (1997).

The important point for this paper is that the majority of monitoring programmes have concluded that pipeflow is a significant contributor to streamflow and that average contributions are commonly in excess of 40%. The response patterns in terms of peak lag times and peak runoff rates per unit of drainage area also tend to fall in-between saturation overland flow and matrix throughflow (Jones, 1997a–d). Pipes are by no means present in all basins and even where pipes are present they may not flow in all storms. Nevertheless, Jones et al. (1997) find that

nearly 30% of the land area of Britain is susceptible to piping. This suggests that current hydrological models that do not attempt to model pipeflow are ignoring a potentially important physical process. Even HOST, the Hydrology Of Soil Types (Boorman et al., 1995), which provided a major upgrade on the UK Flood Studies Report's treatment of soil parameters, does not cover the effects of piping adequately.

1.2. Previous pipeflow models

A number of previous models have been more conceptual than quantitative. These demonstrate certain similarities between different environments as well as some interesting differences. A common feature in many environments is that pipeflow either captures overland flow via sinkholes and macropore inlets or else it benefits indirectly from bypass flow feeding the phreatic surface (Carey and Woo, 2000; Holden and Burt, 2002). The frequent exchange between surface and subsurface routeways is illustrated in the flow diagram developed from field monitoring on the Maesnant by Jones (1987).

A second common element is the concept of pipeflow being controlled by thresholds in soil moisture levels. This is especially clear in the conceptual model produced by Wilson and Smart (1984), but is also used by Gilman and Newson (1980) and McCaig (1983). However, in the subarctic permafrost zone Carey and Woo (2000) noted the importance of frost table depth in their conceptual model. This is analogous to another process more commonly identified in conceptual models: pipeflow initiated by perched water tables created by lower permeability horizons beneath the pipe (Yasuhara, 1980).

Amongst the truly quantitative modelling studies, Gilman and Newson (1980) used a simple parametric lumped linear reservoir model in which up to four parameters were optimised against data from 25 pipeflow hydrographs. The values of the parameters were derived by iterative optimisation using the standard Newton–Raphson method, rather than from direct field measurements of the controlling variables. The most important parameters, 'soil moisture storage in excess of the threshold level needed to initiate pipeflow' and a recession constant, were sufficient to obtain a reasonable fit in most storms, but the others, representing the amount of rainfall passing directly

into the pipes and the amount of leakage loss, were needed for some storms, especially where exceptionally rapid responses were found.

Both Gilman and Newson (1980) and McCaig (1983) also produced empirical models of pipeflow transmission, ignoring the problems of identifying the sources of pipeflow and concentrating solely upon channel flow within the pipe. The former used data obtained from an artificial pump experiment to calculate the coefficients of a kinematic wave model. McCaig based his model on the Chezy formula, making a number of simplifying assumptions such as constant flow at half-full and a linear increase in discharge downslope. These approaches were analysed and compared with data from the Maesnant experiment in mid-Wales by Jones (1988), who found that neither approach was adequate as a general model because of uneven contributions from tributary pipes and effluent seepage along the pipes.

Barcelo and Nieber (1981, 1982) developed a finite difference (time domain) and finite element (space domain) model, which used a two-dimensional adaptation of the Richards equation and the model of Kirkham (1949) for inflow into tile drains. Both saturated and unsaturated zones were present, with a fluctuating phreatic surface. Unlike the models hitherto, this was used purely for computer experiments to test the relative importance of pipe depth, length and network size on pipe discharge, without reference to field data. The five simulations reported showed pipeflow ranging from under 23% of hillslope discharge for a single pipe high in the soil profile to nearly 53% for a large pipe network and deep-seated piping. Clearly, the deeper the piping, the greater the phreatic pressure head and the longer it is maintained, and the denser the pipe network, the better the drainage.

The most elaborate model to date was developed by Nieber and Warner (1991) from the earlier model incorporating a more explicit modelling of the third dimension. This was a finite difference model based on three-dimensional Darcian flow from a saturated soil of uniform hydraulic conductivity into a single, unbranching pipe. The pipe itself was treated as a porous medium rather than a void or channel. This avoids the problem of discretising the boundary of the pipe in the grid mesh and the large number of grid nodes that would result. A number of computer simulations were run to determine the effects of
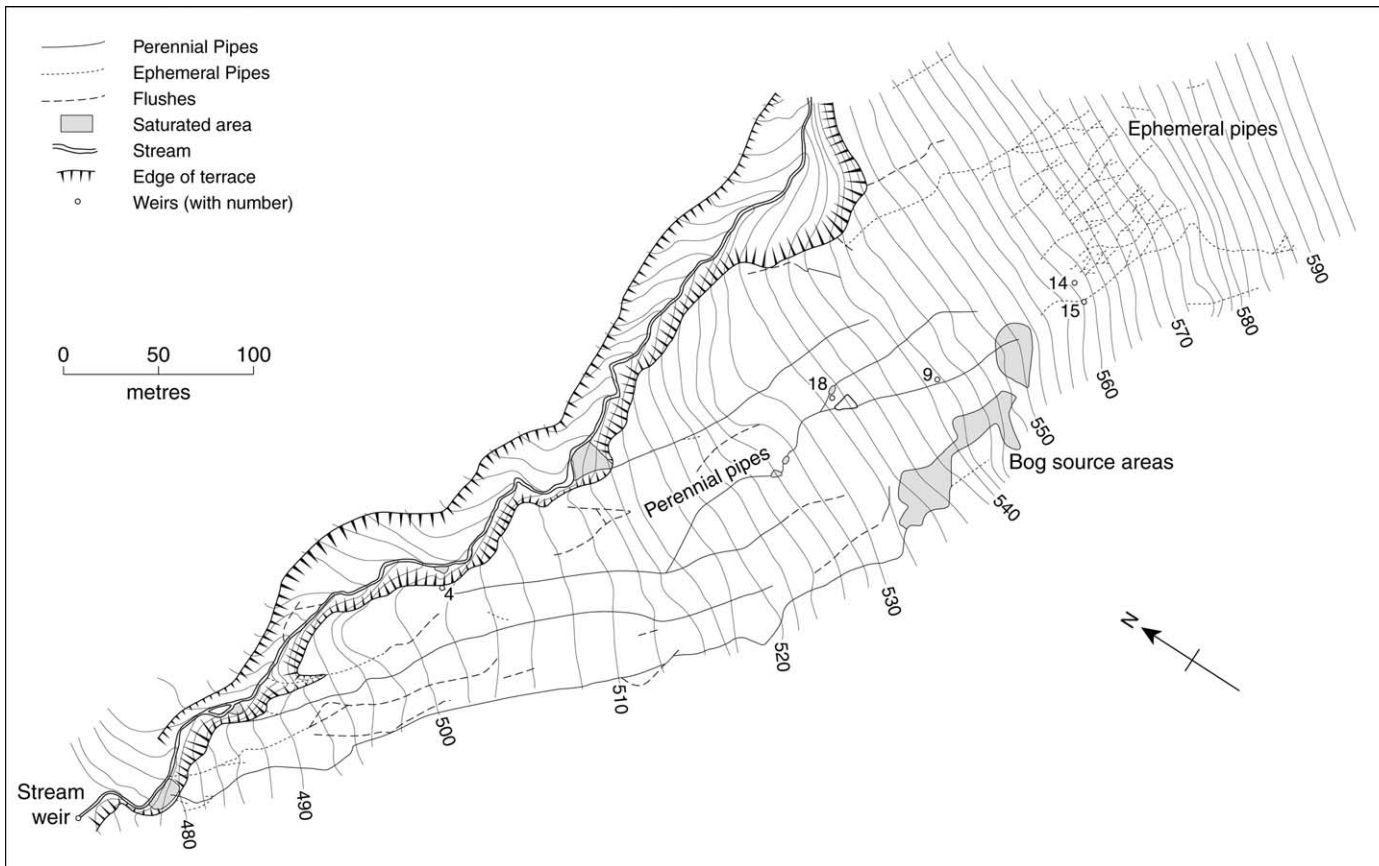
Fig. 1. Map of the main Maesnant pipe network, with locations of monitoring sites for pipeflow and the phreatic surface. The individual pipe reaches used in the semi-distributed simulation model are marked by segments AB, BC, etc.
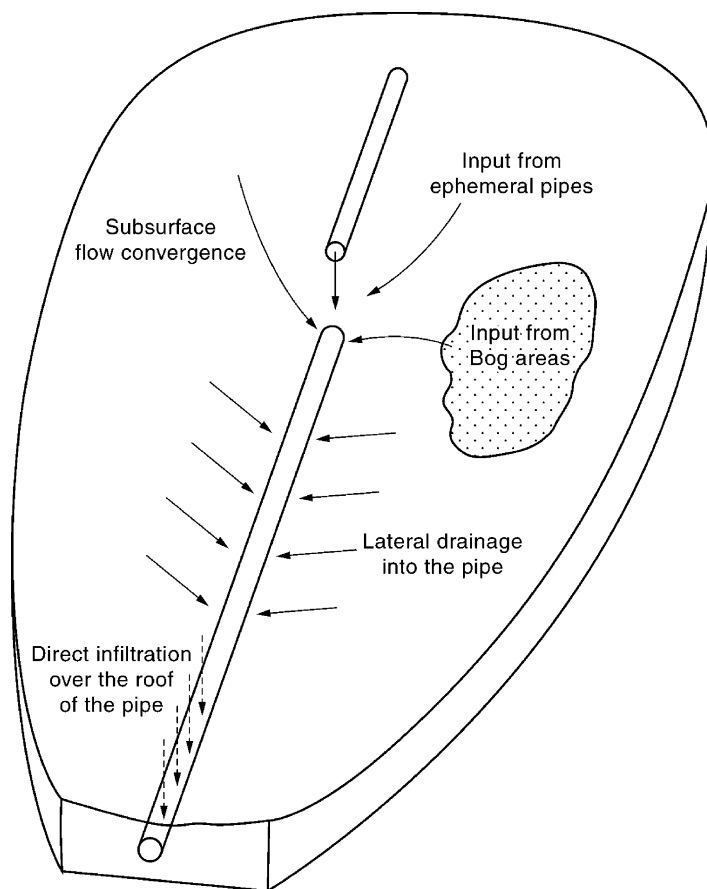
Fig. 2. Conceptual framework of the model showing sources of pipeflow.

altering pipe depth, radius, length and spacing, and slope angle and length. The simulations produced some interesting results, especially the suggestion that there may be thresholds in the relative importance of pipeflow versus throughflow, which depend on the depth of piping and its upslope extension relative to the width of slope. For example, simulations using slopes that were longer than they were wide, showed pipeflow could become dominant once the pipe extended over more than three-quarters of the length of the slope.

However, the remit of Nieber and Warner's experiment also limits its applicability. Like Nieber's earlier experiment, it was not related to a specific field case and was not compared with field data. More importantly, the analysis was purely concerned with subsurface drainage processes, but the assumptions of the model meant that there was continuous saturation overland flow throughout each simulation. The authors' summary table shows that pipeflow is insignificant, accounting on average for little more than 1% of total hillslope discharge compared with 22% from matrix throughflow and 77% from overland flow. These results are the consequence of having to maintain saturated soils throughout the slope in order to simplify the modelling.

The authors might have obtained more realistic results by examining transient saturated–unsaturated flow rather than just steady saturated conditions. In the real world situation, steady state flow is rare and dynamic conditions prevail. This can be illustrated from the data collated from a wide variety of field experiments presented by Dunne (1978), Kirkby (1985), Anderson and Burt (1990) and Burt (1992)

on overland flow and throughflow and by Jones (1997a,b,c) on pipeflow. For example, taking the largest catchment in Nieber and Warner's simulations with an area of $1200 \, m^2$ $(0.0012 \, km^2)$ their results indicate that 94% of rainfall drains via overland flow, 1.2% by throughflow and 1.6% in pipeflow. However, interpolating from the Dunne–Jones field data for a catchment area of $1000 \, m^2$ indicates typical mean runoff coefficients of only 35% for Hortonian overland flow, 10% for throughflow and 56% for pipeflow (Jones, 1997b).

The discrepancies are even greater when the model results are compared with the flowchart of drainage routes during the average (30 mm) rainstorm on the Maesnant itself, presented by Jones (1987). This indicates an overall runoff coefficient of 68%, which is broken down between 44% via pipeflow, 21% via throughflow and 3% from saturation overland flow.

2. The model

The aim has been to develop a general model of pipeflow that can be applied to both perennially and ephemerally flowing pipes in a variety of locations. With this in mind, the objectives have been (i) to develop a model that is as physically based as possible, so that it can be applied to different pipe networks simply by changing the physical parameters of the environment and the network, and (ii) to test and refine it by using the model to simulate pipeflow hydrographs which fit the field data for the Maesnant basin. The model is designed to be used as a storm-flow event model.

The Maesnant basin has extensive networks of ephemerally flowing pipes, but the bulk (on average 88%) of the contribution to the stream from these ephemeral pipes passes through larger and deeper perennially flowing pipes downslope of the area of most intensive ephemeral piping (Fig. 1), i.e. only 12% of ephemeral pipeflow issues directly into the stream (Jones and Crane, 1984; Jones, 1987). Unlike most previous models, which have been limited to ephemeral pipes, this model is intended to be a universal model for both types of pipeflow regime. The conceptual framework, based upon more than a decade of observations in the basin, is shown in Fig. 2.

The model recognises two sources of pipeflow:

(a) an upslope supply area feeding the head of the pipe, and
(b) limited areas orthogonal to the long axis of the pipe.

For the perennially flowing pipes, the upslope supply areas are mid-slope bogs where resurgent groundwater mixes with direct precipitation on the bog surface and occasional contributions from the network of ephemerally flowing pipes higher up the slope. If the model is applied solely to the ephemeral network, the upslope supply comes from overland flow and rapid seepage, either from peat surfaces with low infiltration capacity or from scree slopes and gravelly rankers. In both cases, there is a rapid runoff response dominated by overland flow entering cracks or pipeheads and supplemented by saturated throughflow. Most overland flow is saturation overland flow, although some localised Hortonian overland flow may feed the heads of ephemeral pipes.

There is, therefore, some similarity between the perennial and ephemeral networks in terms of the generation of water supply at the pipehead. The differences in response are due mainly to groundwater levels and the consequent differences in the frequency of saturation at and above the depth of the pipe.

Rising and falling phreatic levels are also the main controlling factor for the second source of supply along the length of the pipes for both perennial and ephemeral networks. The ephemeral pipes respond to approximately one in every three storms that generate stormflow in the perennial pipes because of lower phreatic surfaces relative to pipe level in both the upslope and the lateral source areas. The phreatic surface is perennially above the bed of the pipe in the perennially flowing pipes so that they have a permanent baseflow. Lag times between rainfall and the initiation of stormflow in the perennial pipes tend to be shorter than in the ephemerals because of this ready primed state, so that although peak flows tend to migrate down the networks from the ephemerals to the perennials in the usual way for stream channels, initial response tends to start at the outfalls of the perennials and work upslope (Jones, 1988).

Fig. 3 shows a flowchart for the simulation model written in FORTRAN 77. It takes the form of a

Subroutine for perennial pipes

```
Input number of pipe segments
            ↓
Read geometric properties
            ↓
Input pre-storm water table (WT) & sensitivity to rainfall
            ↓
Calculate width/depth of pre-storm flow
            ↓
Enter start time of storm
            ↓
Read rainfall by time interval
```

Rain>0? — No → Q>baseflow? — No

Rain>0? ↓ Yes

Q>baseflow? ↓ Yes

WT rise	WT falls rate A	WT falls rate B
↓	↓	↓
Wetted perimeter increases	Wetted perimeter decreases at rate A	Wetted perimeter decreases at rate B
↓	↓	↓
Effluent seep increases	Effluent seep decreases at rate A	Effluent seep decreases at rate B

```
Calculate discharge (Q) & store
            ↓
Increment time interval
            ↓
end of rain?  → No
     ↓ Yes
More segments? → Yes
     ↓ No
Go to flow collation and routing
```
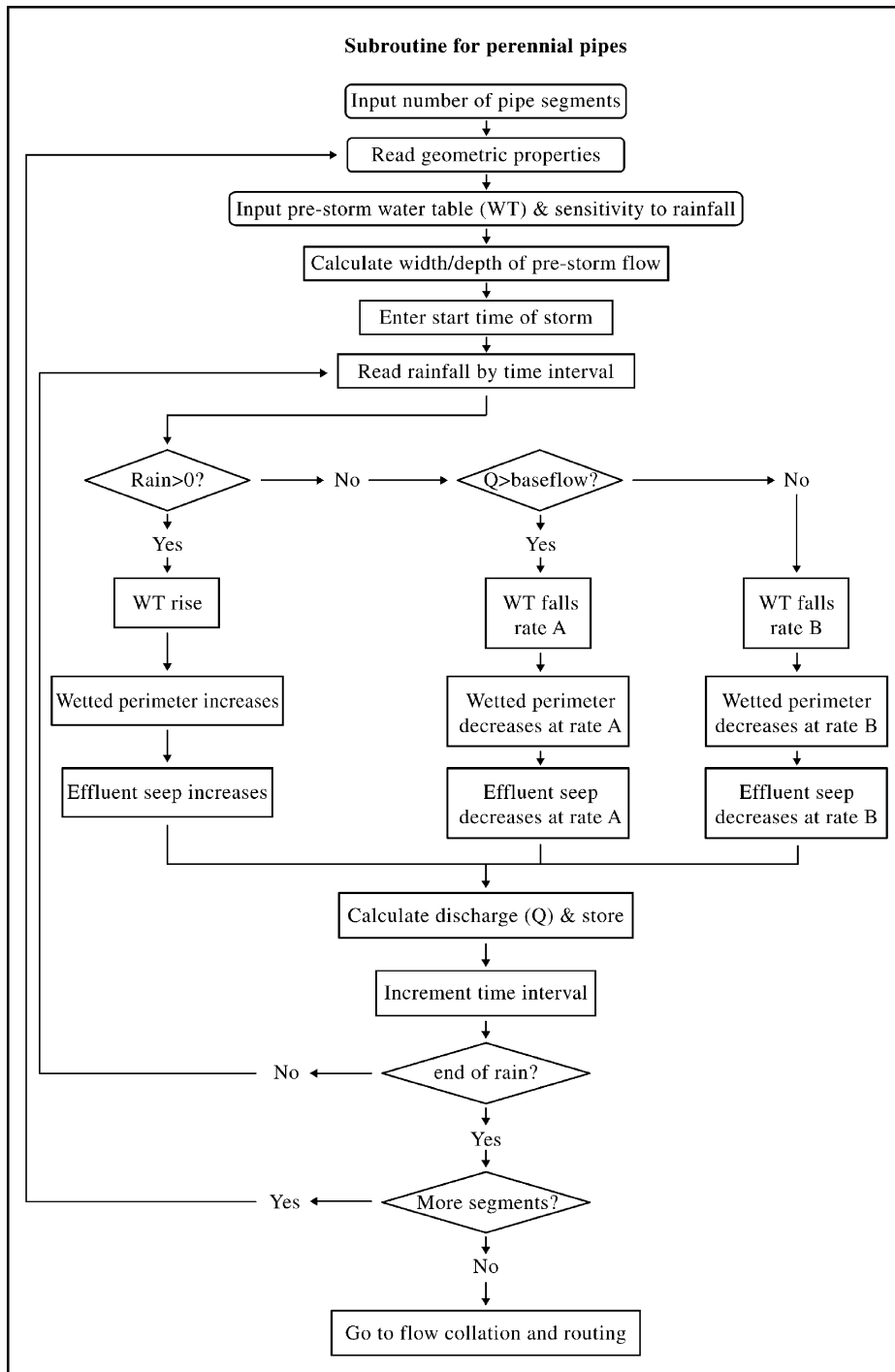
Fig. 3. Flowchart of the simulation model. The three subroutines calculate input from the three main sources of pipeflow (ephemeral pipes, bog and perennial pipes), which are collated and routed by the final algorithm. (Abbreviations: WT is the phreatic surface, $\sum$Rain is accumulated rainfall, smc is soil moisture content, and Q is discharge.)
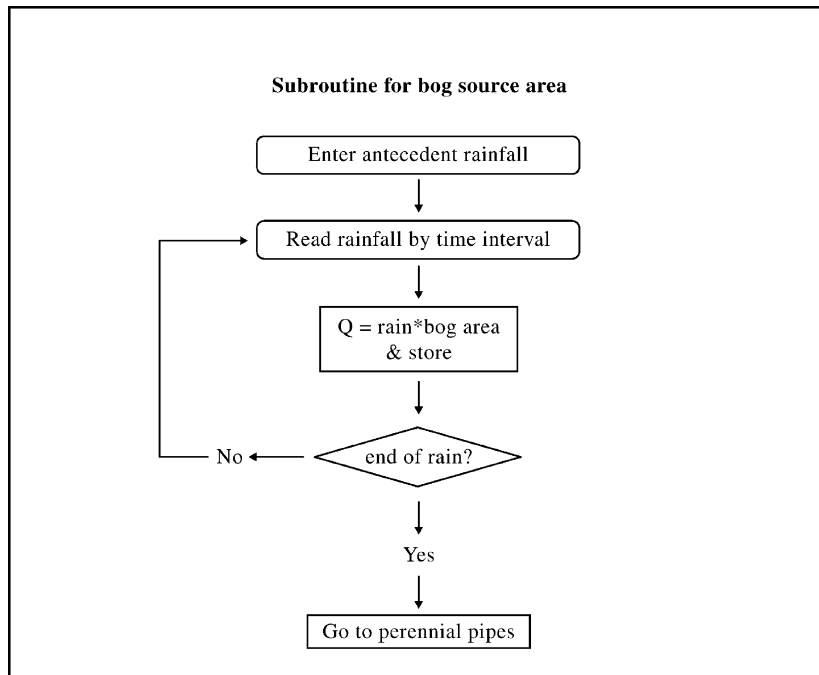
Fig. 3. (*continued*)

parametric conceptual model in which the parameters are all closely related to the physical processes deemed to be responsible for controlling pipeflow (Connelly, 1993). A semi-distributed approach has been adopted, whereby the pipe network is divided into a number of reaches in which the local properties of the soil, pipe geometry and flow sources are modelled separately and later combined.

More elaborate submodels could be incorporated at a later stage, for example, to model infiltrating water using the Richards equation and a macropore flow model. However, this would require more calibration data to be collected than was judged reasonable at this stage, considering the high degree of spatial variability in infiltration capacity and hydraulic conductivity revealed by surveys using a Guelph permeameter and a double-ring constant head infiltrometer, and the sensitivity of flow through these small pipes (averaging 93 mm diameter in the ephemerals and 240 mm diameter in perennials) to this heterogeneity. Matrix infiltration capacity was found to vary by up to three orders of magnitude within a distance of 50 m without any allowance for the effect of numerous cracks, which are

consciously avoided in the standard methods of measurement (Jones, 1990).

Calculations based on these measurements also indicated that if rainwater were infiltrating solely via matrix routes, it would take far longer to reach pipe level than the observed response time of the pipes. In most cases, the infiltrating rainwater would reach the pipe well after peak discharge or even after the end of stormflow. This underlines the dominance of crack or macropore flow in transmitting rainwater to the pipes. However, the process is probably indirect, since too little rainwater will fall directly onto the roofs of pipes. Either the cracks are entrapping overland flow or they are directing water to the phreatic surface whence it drains into the pipes.

The dipwell and piezometer records prove that phreatic levels rise for up to 15 m on either side of the main pipe at the same time as pipeflow commences, which creates hydraulic gradients towards the pipe of 0.5 m or more in 10 m (Fig. 4). Sklash et al. (1996) have concluded from isotope studies in a nearby basin that phreatic water is the main supplier of pipeflow. In reality, this may indicate either old water displaced by piston flow or a mixture
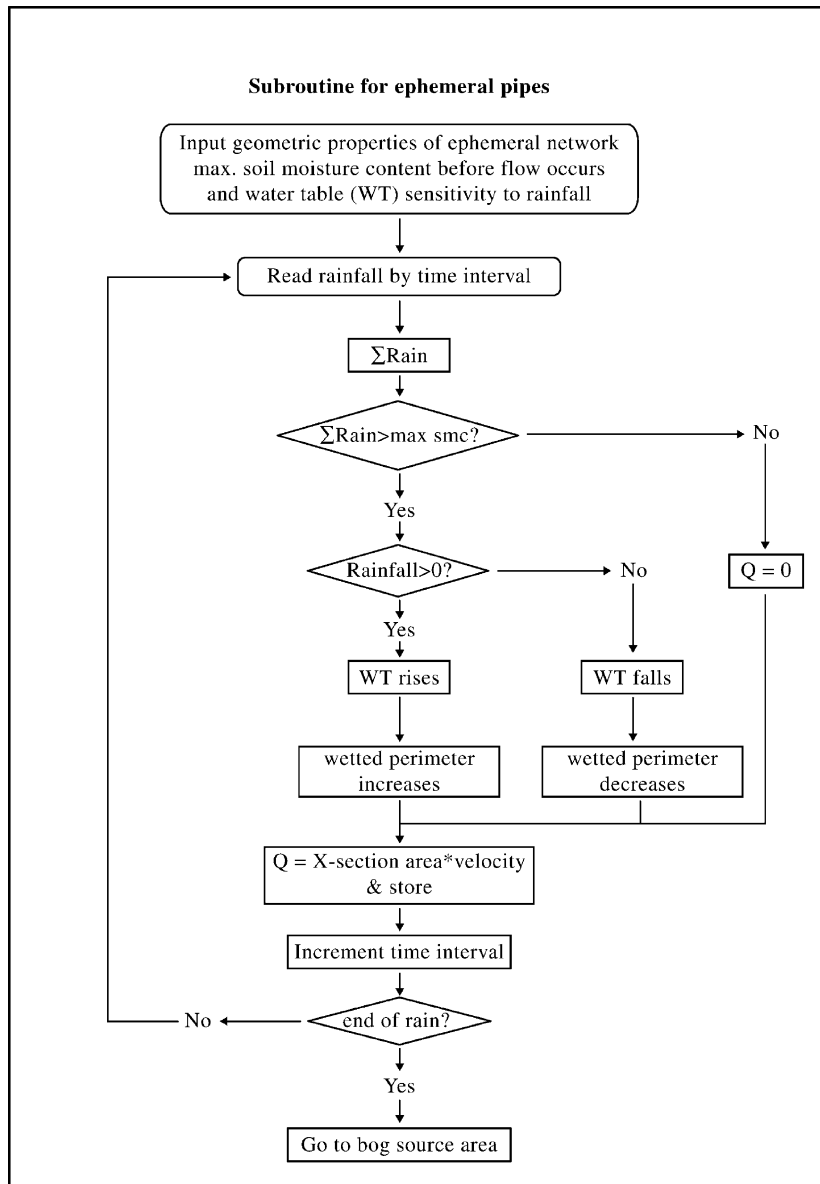
Subroutine for ephemeral pipes

Input geometric properties of ephemeral network
max. soil moisture content before flow occurs
and water table (WT) sensitivity to rainfall

Read rainfall by time interval

ΣRain

ΣRain>max smc? — No

Yes

Rainfall>0? — No   Q = 0

Yes

WT rises   WT falls

wetted perimeter   wetted perimeter
increases   decreases

Q = X-section area*velocity
& store

Increment time interval

No — end of rain?

Yes

Go to bog source area

Fig. 3. (*continued*)

of old and new water from the current rainstorm within the groundwater.

In the absence of a detailed knowledge of crack or macropore networks, phreatic levels were estimated from rainfall based on regression equations derived from the field dipwell measurements. Phreatic levels were monitored at 24 dipwells in five sets laid perpendicularly across the line of the pipes, supplemented by

rectangular banks of manually read piezometers (Fig. 1). Eighteen of the dipwells were logged at 10 min intervals on Tinylog solid state data loggers attached to specially designed float and potentiometer sensors (Jones et al., 1984). In the model, phreatic levels at the start of each storm were set according to an empirical relationship established with the 7-day antecedent rainfall. During the course of each storm, phreatic
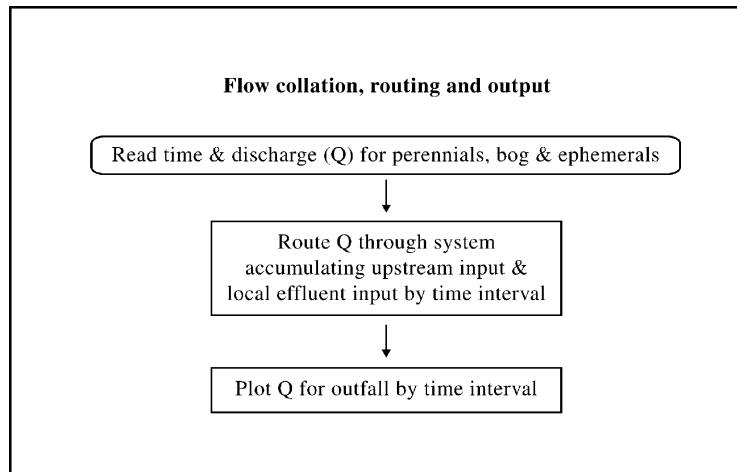
Flow collation, routing and output

Read time & discharge (Q) for perennials, bog & ephemerals

Route Q through system
accumulating upstream input &
local effluent input by time interval

Plot Q for outfall by time interval

Fig. 3. (*continued*)

levels fluctuated in response to the pattern of rainfall. The average rate of rise per unit of rainfall was calculated for the rising limb of the pipeflow hydrograph by dividing the maximum height of rise in the water table by the total storm rainfall prior to maximum phreatic level. Similarly, the total downward movement of the water table during recession was divided by the time since the last rainfall to give an average rate of fall. In the ephemeral pipes, the equation allows the phreatic surface to fall below the bed of the pipes, whereas the equation for the perennial pipes does not. The level to which

it falls in the perennials was determined on a seasonal basis from long-term baseflow records collected in the previous study programme (Jones and Crane, 1984).

One-third of the data was used to develop empirical equations and these were then tested on the remainder. Comparison of the predicted patterns of water level movement with the recorded dipwell sequences generally showed a very good fit, with correlations of better than $r = 0.9$, which justified the procedure, at least as a first step. The best fit equation for the fall of the water table under average
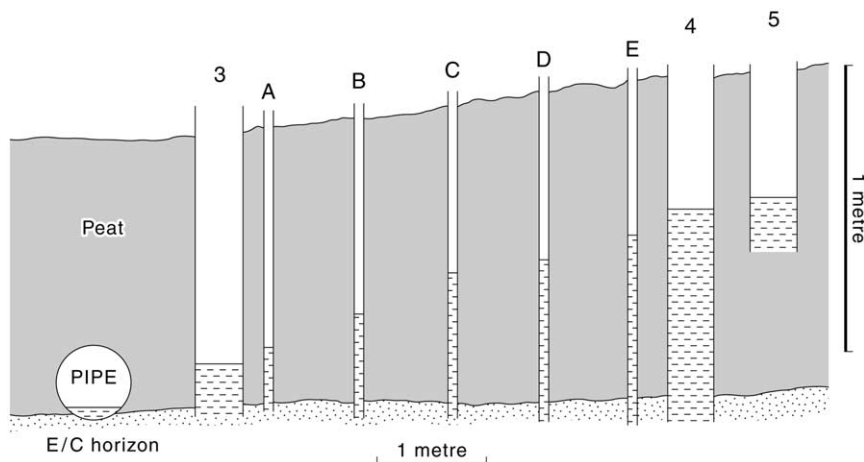

Fig. 4. Hydraulic drawdown and gradients around the master pipe measured by a dipwell and piezometer transect. Letters A–E indicate piezometers, numbers indicate dipwells.
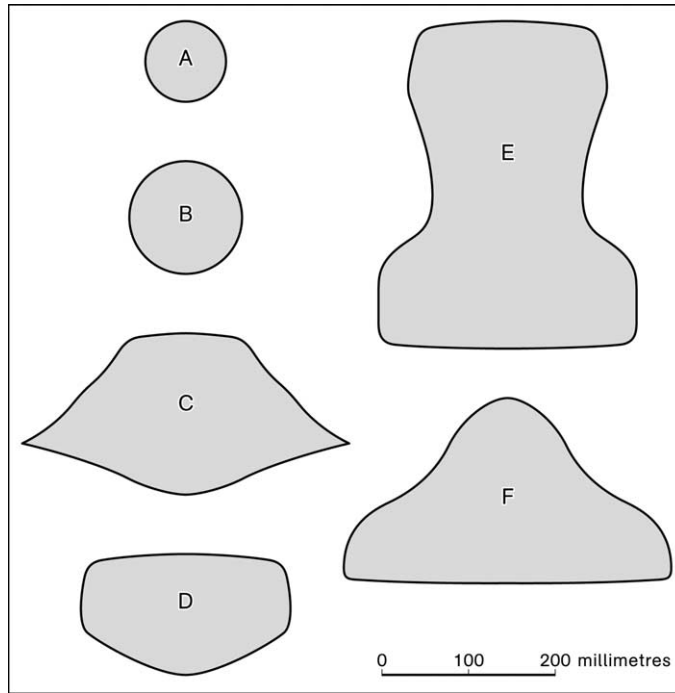
Fig. 5. Sample cross-sections of Maesnant pipes; A is a typical ephemeral pipe, B the head of the perennial network, C–E are progressively downslope along the modelled pipe, number 4 in Fig. 1, and F is on pipe 2.

conditions was

$$d_{w(t+1)} = d_{w(t)}^{-1.005} \tag{1}$$

where d_w is the depth of the phreatic surface and t is the time point, $t + 1$ being the next discrete time point.

The orthogonal supply of seepage water along the pipes is controlled by (i) the lateral hydraulic conductivity of the soil, (ii) a variable hydraulic gradient created by the divergent effects of maximum phreatic levels in the area between the pipes and drawdown at the pipe boundary, and (iii) the area of the pipe boundary that is below the phreatic surface. The amount of water entering the pipe is calculated by an equation of the form:

$$Q = W.U.L \tag{2}$$

where Q is the rate of discharge of seepage water into the pipe, W is the wetted perimeter of the pipe, U is the velocity at which water enters the pipe, and L is the length of the pipe.

The velocity of seepage into the pipe, U, is deter-

mined by Darcy's Law from measured hydraulic conductivity and from hydraulic gradients that were calculated from the observations at the banks of dipwells and piezometers located in Fig. 1. Saturated hydraulic conductivities in each soil horizon were measured in the field with a constant head model 2800K1 Guelph permeameter and surface infiltration rates in the peat were measured with a single-ring falling head infiltrometer.

The model divides the pipe network into segments or reaches. A reach is defined as a segment of pipe along which there is a reasonable uniformity in average pipe geometry and slope. The hydraulic conductivity values entered into the model are weighted according to the proportion of the soil profile in the different horizons in each reach of the pipe network, based on the depth of the pipe bed and the dimensions of the pipe cross-section.

Hydraulic gradients were calculated from the empirical estimates of phreatic levels at the pipe boundary and at the distance of the furthest ground-water monitoring site from the pipe or the peak level
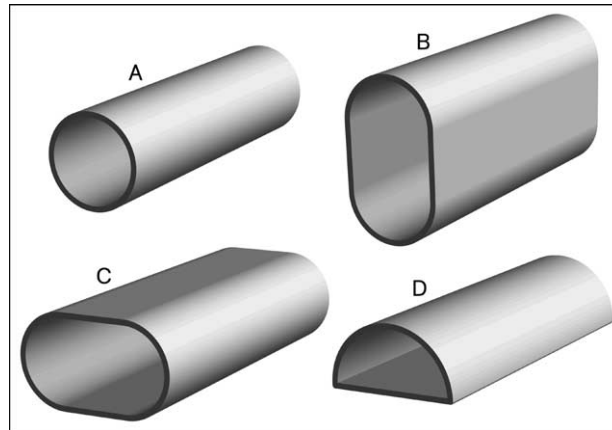
Fig. 6. Simplified geometry of pipe cross-sections used in the model. Sample combinations of circular and rectangular elements.

in the phreatic surface, whichever is the shorter. The area of effluent seepage on the bed and walls of the pipes was calculated by geometry for an average cross-section of pipe in each reach and the same empirically estimated phreatic levels. Fig. 4 illustrates a typical pattern of phreatic levels around the pipe.

The wetted perimeter, W, over which water can enter the pipe is a function of the depth of the phreatic surface and the geometry of the pipe. The relationship can be expressed in general form as

$$W = f(H, C_1, C_2, ..., C_n) \qquad (3)$$

where f is a function, H is the height of the phreatic surface above the bed of the pipe and the Cs are parameters of the cross-sectional geometry of the pipe, e.g. diameter.

The shape of the pipe cross-section may have an important effect on lateral inflow, as well as on frictional resistance to flow within the pipe. It will affect the rate at which the wetted perimeter increases during stormflow and therefore potentially affect the rate of effluent seepage into the pipe as the phreatic surface rises, especially if the shape cuts through horizons of differing permeability. Most pipe cross-sections do not match the ideomorphic circular form assumed by Nieber and Warner (1991) or McCaig (1983) in their models. Indeed, they are quite variable, as shown in Fig. 5 from Maesnant and by the fibre-scope probe study of Terajima et al. (2000). Jones (1981) classified the cross-sections of 172 pipes in three contrasting basins as circular, horizontally

lenticular and vertically lenticular. In the upland basin of Burbage Brook in the English Pennines (mean altitude 357 m) 40% of the 138 pipes surveyed were horizontally lenticular, 34% circular and 26% vertically lenticular. In contrast, on Afon Cerist in North Wales (mean altitude 150 m) 70% were vertically lenticular, 18% circular and only 12% horizontally lenticular, whilst, in the lowland basin of Bourn Brook, Cambridgeshire (46 m) circular forms predominated (76%), with the remainder all horizontally lenticular.

Horizontally lenticular forms often take on an upturned 'D' shape with a flat bed, which has been commented upon by numerous writers in many parts of the world (Ward, 1966; Conacher and Dalrymple, 1977). This form would result from selective erosion in a partially filled pipe and it is a further evidence against the notion that pipes constantly flow full to capacity, which has been the standard assumption in modelling to date (Nieber and Warner, 1991), or even constantly half-full, as assumed by McCaig (1983). A pipe with a broad base will tend to admit more water than one with a narrow base when the water table is only just above the pipe bed, provided the permeability of the perimeter is uniform. Conversely, vertically lenticular cross-sections tend to be more common where there is a steep hydraulic gradient along the line of the pipe and active downcutting of the bed. They also tend to be larger. In the Maesnant experimental basin, headwater ephemeral pipes tend to be small and circular, and perennial pipes on the lower

slopes tend to be larger and more vertically lenticular as they approach their outfalls on the edge of the river terrace (Figs. 1 and 5).

Vertically lenticular pipes are more likely to span a variety of soil horizons. Hydraulic conductivities are often higher in the layer immediately above the pipe bed (Jones, 1981, figs. 10 and 11). Pipes typically flow through an erodable, open-textured horizon above an impeding layer (Jones, 1981, 74ff; Jones, 1971). On Maesnant, the perennial pipes flow in a more permeable layer above an impermeable clayey substrate of solifluction drift and the hydraulic conductivity of the bed and lower walls is more than 60 times that of the roof and upper walls where these are in peat (0.609 against 0.009 mm s^{-1}, Jones, 1981, p. 81). Hence, shape and size can affect the mean hydraulic conductivity of the pipe circumference as well as the extent of the wetted perimeter.

In the current simulations, the main pipe was divided into four reaches at the dividing points A–E in Fig. 1. The model allows the average cross-section in each reach to be represented by two simple geometric shapes, a circle (or semicircle) and a rectangle, either singly or in any combination. Fig. 6 shows the most likely combinations. Each element in the combination can be sized to fit individual pipe segments.

Pipehead supplies for the perennial pipes were calculated from three elements: (i) output from the ephemeral pipes, (ii) precipitation falling directly onto the surface of the mid-slope bog areas located at the break of slope between the drift terrace containing the perennial pipes and the rock-based hillside above it (Fig. 1), and (iii) groundwater resurgence at this point. The input from the ephemeral network is modelled by varying the length of contributing pipes in relation to the estimated prestorm height of the water table. The real-world transfer from these ephemeral pipes into the perennial network on Maesnant is either by a short run of overland flow or through the upper part of the bog area (Fig. 1), but adding extra length to the ephemeral pipes to cover this section of hillslope proved adequate in the model.

The contribution from direct precipitation is calculated from the rainfall record and the measured surface area of the bogs. The area of bog vegetation is 30 m^2, but the surface area of the bog that contributes runoff is variable. Detailed observations of the

area of bog contributing saturation overland flow were made over a 2-year period. Under very dry antecedent conditions, little or no surface runoff was observed. In these conditions, the contribution from the bog area was excluded from the simulation of stormflow in the perennial pipes. It was assumed that if no overland flow is generated from an area of the bog, then this area would only contribute drainage water to baseflow in the perennial pipes. In extremely wet conditions approximately 50% of the area mapped as *Sphagnum* flush vegetation contributed overland flow. The equation covering channel precipitation on the surface of the bog therefore takes the form:

$$Q = b.A.R \tag{4}$$

where A is the total area of the pipehead bog, R is total storm rainfall and b is a runoff coefficient. The coefficient represents the area of saturated bog surface. The model directs one of five values to be selected, depending on the 7-day antecedent rainfall, based on the long-term field observations of the extent of the saturated bog surface. The maximum value of 0.5 is assigned when weekly antecedent precipitation exceeds the long-term weekly average of 50 mm. This is then progressively reduced in steps of 0.1 at threshold values of 35, 25 and 15 mm.

The amount of groundwater resurgence is more difficult to estimate. Much of this flow is quite deep and seems to flow through the greywacké and mudstone bedrock, perhaps in discrete pathways of unknown length and complexity. Some indication of the problem was found when we tried to determine the source of flow at the very head of the ephemeral network by excavation. Even there, water welled up from a fissure in the bedrock. This is reminiscent of the case reported by Stagg (1974) of soil piping and rilling heading in bedrock springs in sandstone on the Black Mountains in South Wales.

Because of the difficulties in assessing the amount of resurgent groundwater, an empirical estimate was made by using the measured discharge at the nearest point to the outfall of the bog area (site 9 on Fig. 1). By subtracting from this the contributions from the ephemeral pipes monitored at sites 14 and 15, together with the calculated direct rainfall contribution to the bog surface, the remaining discharge provided an estimate of groundwater contributions that could be correlated with total storm rainfall.

Table 1
Comparison of observed and simulated stormflow discharges at the outfall of pipe 4 in the Maesnant experimental catchment (NS—no significant difference between simulated and observed by χ^2)

| Storm number[a]	Season	Start date (Julian day)	Total rainfall (mm)	Peak intensity (mm h^{-1})	Storm duration (h)	Observed discharge (m^3)	Simulated discharge (m^3)	Simulated as percent of observed	Objective function	χ^2 statistic	Degrees of freedom	Significance level
Calibration storms												
1	Spr	67	37.0	5.5	14.0	461.295	412.295	89.4	0.2274	9.714	36	NS
3	Win	342	43.0	4.5	16.1	286.235	261.792	91.5	0.0562	7.093	41	NS
12	Spr	118	18.5	3.0	10.1	98.931	93.737	94.8	0.1299	7.874	29	NS
17	Win	357	17.5	6.0	5.0	278.884	256.521	92.0	0.0717	5.072	28	NS
19	Aut	324	13.0	4.9	11.5	661.134	621.251	94.0	0.0474	30.698	39	NS
Simulation storms												
2	Spr	72	16.5	4.0	13.0	721.695	696.405	96.5	0.0441	4.545	28	NS
4	Aut	256	42.5	4.5	13.2	98.168	90.297	92.0	0.0796	4.476	30	NS
5	Win	48	60.0	5.8	26.4	115.509	117.237	101.5	0.0364	1.840	34	NS
6	Spr	131	16.5	1.5	18.0	167.349	167.426	100.1	0.0527	5.919	31	NS
7	Spr	82	33.5	5.3	14.2	115.679	119.765	103.5	0.0454	2.700	20	NS
8	Win	11	20.0	5.7	7.7	226.397	250.729	110.8	0.0663	5.650	26	NS
9	Win	16	15.5	6.6	4.6	132.048	159.880	121.1	0.0693	8.073	34	NS
10	Win	13	29.0	7.2	13.8	229.075	240.110	104.8	0.0289	1.819	31	NS
11	Aut	334	42.0	4.5	23.0	189.066	227.364	120.3	0.0479	5.336	31	NS
13	Spr	79	24.5	5.2	23.8	235.565	233.449	99.1	0.0002	0.013	16	NS
14	Win	45	19.5	6.8	7.7	341.645	342.217	100.2	0.1131	10.695	38	NS
15	Win	20	9.0	1.8	16.6	673.571	670.890	99.6	0.0317	2.488	22	NS
16	Spr	76	56.0	5.1	35.3	155.127	150.521	97.0	0.0584	2.087	31	NS
18	Win	354	11.0	7.9	4.6	84.100	83.161	98.9	0.0248	1.365	35	NS
20	Aut	297	18.0	2.2	17.0	387.803	382.489	98.63	0.0561	47.583	37	NS

[a] In order of observation.
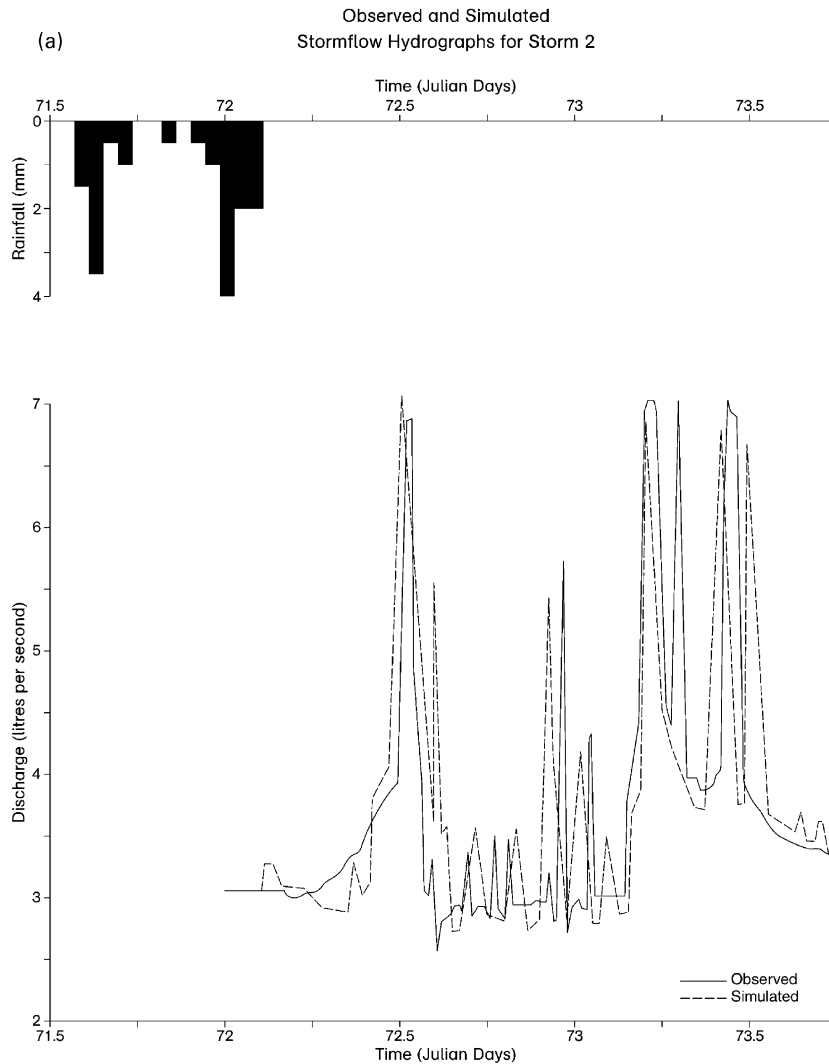
Fig. 7. Examples of pipeflow simulations compared with recorded pipeflow: (a) storm 2, (b) storm 6, (c) storm 8, and (d) storm 16. See Table 1 for details and the text for explanations. (Note hyetographs are not plotted hourly.)

The model accumulates inputs along the known length of pipe on a reach by reach basis, combining input from upslope reaches and lateral contributions within the reach. This is routed from one reach to the next downstream based on estimated velocities of flow. Velocities, V, were estimated from dye dilution experiments, which allowed the following relationship to be established with pipeflow discharge, Q:

$$V = 0.0025Q^{0.743} \tag{5}$$

The contribution from a tributary pipe was monitored at site 18 (Fig. 1). It was found that this extra contribution could be adequately modelled by increasing the size parameters of the receiving reach, thus obviating the need for explicit modelling of pipeflow in the tributary. This simplification would probably not have been sufficient if the pipe network had more tributaries. In that case, the number of reaches in the model would have to be increased in order to model the tributaries in detail.
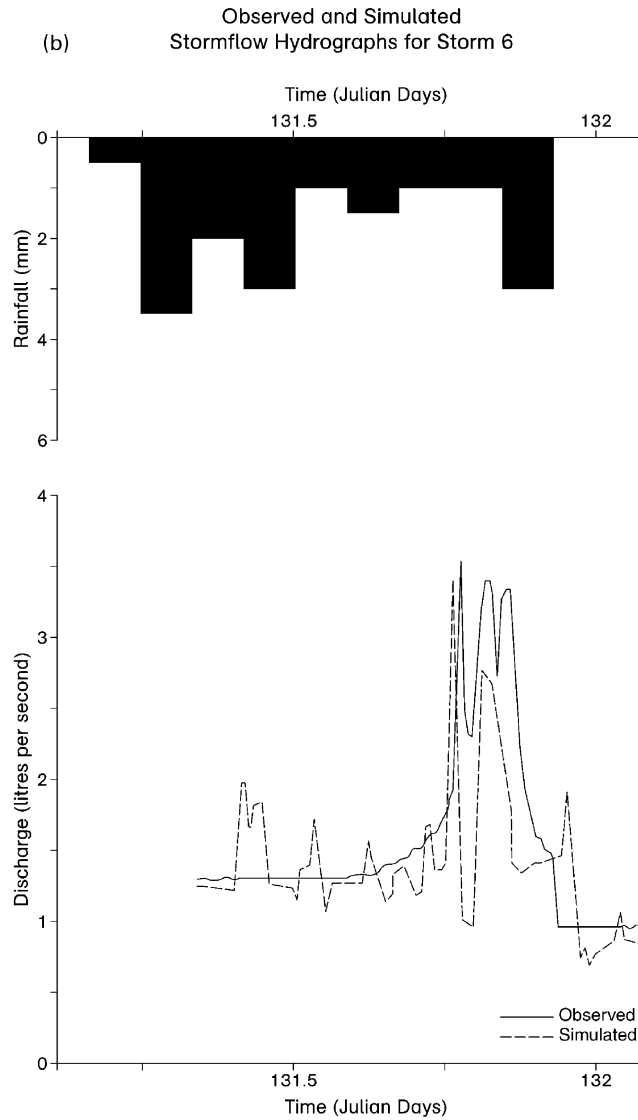
Fig. 7. (*continued*)

2.1. Calibrating the model

The model was calibrated using the pipeflow and dipwell data recorded at five sites along the largest ephemeral–perennial network on Maesnant with its outfall at site 4 (Fig. 1). Pipes were locally excavated and the water-level sensors set in stilling wells in the pool behind miniature combined V-notch and rectangular weir plates. Monitoring lasted 15 months. This was in addition to 30 months of continuous pipeflow

data collected at four of the sites from a previous monitoring programme (Jones, 1987). Rainfall was measured near the lower stream weir (Fig. 1) by an Institute of Hydrology ground level 0.5 mm tipping bucket and logged at 5 min intervals. A total of 20 complete storm hyetographs and hydrographs were used for calibrating and testing the model.

For the storms selected to calibrate the model, optimisation was achieved by adjusting the model parameters where necessary in order to minimise the
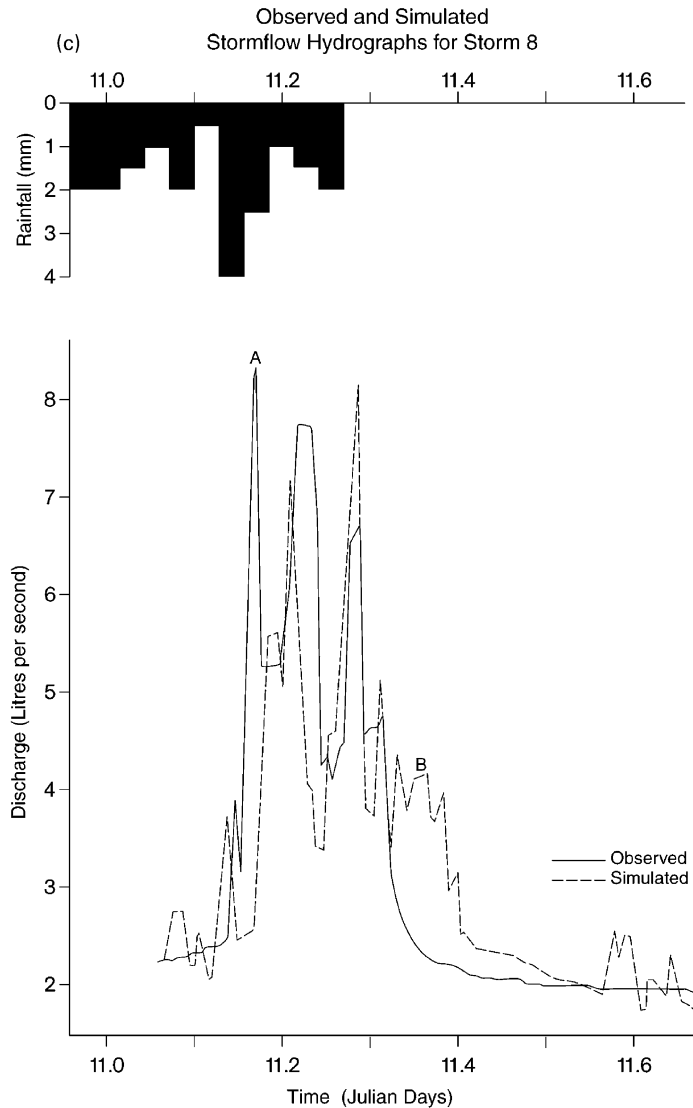
Fig. 7. (*continued*)

objective function, F:

$$F = \frac{\sum_{i=1}^{n}\left(\left(Q_i \sum_{j=1}^{n} P_j Q_j / \sum_{j+1}^{n} Q_j^2\right) - P_i\right)^2}{\sum_{j=1}^{n} P_j^2} \qquad (6)$$

where P_i are the measured instantaneous pipeflow discharge values and Q_i are the corresponding simulated pipeflow discharges, and n is the total number of 10-min interval instantaneous logger records in each hydrograph.

3. Results and discussion

The model was calibrated on five storms and used to simulate 15 other storms at the pipe outfall at site 4 (Fig. 1). The storms were spread over the year with the
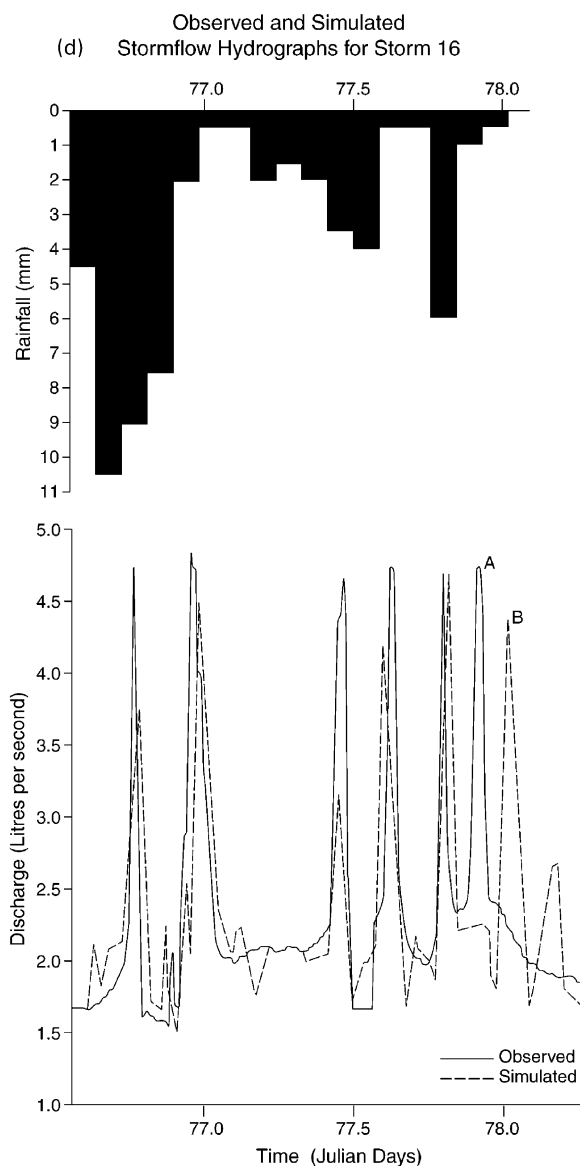
Fig. 7. (*continued*)

exception of summer, for which too few flow records were available. This was partly because flows were very low in summer and partly because desiccation of the surrounding peat can cause leakages and maintenance problems at the pipe weirs.

The simulated storm hydrographs were compared with the observed hydrographs using the objective function, F, to measure goodness of fit. Table 1

lists the total observed and predicted volumes of stormflow for the calibration storms and the test simulations, along with the objective functions. The final three columns of the table list the χ^2 statistic, degrees of freedom and significance levels. None of the simulations were significantly different from the observed pattern of pipeflow and all of the objective function values were low, with an average value

of $F = 0.0503$ for the non-calibrated events indicating a close fit.

Fig. 7 compares a number of predicted pipeflow hydrographs with actual flows. Storm 2 (Fig. 7(a)) is a moderate, twin-peaked storm with a maximum intensity of 4 mm h^{-1} falling on wet ground in early spring. The model matches the hydrograph peaks fairly well, although the final two peaks are delayed by 1–3 h. Storm 6 (Fig. 7(b)) is a longer event in late spring with a maximum intensity of only 1.5 mm h^{-1} falling on a drier catchment. There is a lag time of about 8 h in response at the pipe outfall, but the model feeds through a few minor pulses of around 0.5 l s^{-1} before the main response. The overall fit is not bad and total discharge is perfectly estimated, but the model allows pipeflow to begin a little earlier and produces slightly smaller peaks. Storm 8 (Fig. 7(c)) is a short, moderately heavy winter storm falling on wet ground with a peak intensity of 5.7 mm h^{-1} and a lag time of only 2.5 h between the start of rain and pipe response. Total pipeflow is overestimated by nearly 11% and the very short early peak in pipeflow (point A in Fig. 7(c)) is missed. The next two peaks are modelled reasonably well, but recession discharges are overestimated (point B in Fig. 7(c)). The model has not quite kept up with the speed of response in the real event. Storm 16 (Fig. 7(d)) is a very long and heavy rainstorm with a number of peaks. The model does remarkably well in following the varied pattern of pipeflow, although most of the brief peaks are slightly underestimated and the last gets delayed by a couple of hours (points A and B in Fig. 7(d)). Total discharge is estimated within 3%.

Overall, the principal hydrograph peaks are generally well simulated. The main shortcomings seem to be (i) slightly more erratic response in the simulated flows, and (ii) some brief spikey peaks in the pipeflow seem to be slightly delayed in the simulated flows. The first of these problems could be due to a lack of damping within the model and a simplified approach to flow routing, whereby flow increments occur only at the end of each pipe segment. Treating the shallow phreatic water and groundwater body as a storage reservoir and more continuous flow routing should improve this. As for the timing discrepancy in brief peaks, often recorded in only one or two of the 10-min interval loggings, it seems more a measure of success that they were simulated at all. Even so, some

problems with timing may be due to the fact that this is an event model which does not attempt to simulate antecedent conditions. These are estimated solely on the basis of the total 7-day antecedent rainfall. This simplification probably gives less emphasis to rainfall events of the last day or two than they should have.

The model has achieved a credible simulation of the pipeflow yield at the outfall of the largest pipe network in the test basin. The goodness of fit for the simulated hydrographs is comparable to the average of $F = 0.0565$ achieved by Gilman and Newson (1980) using their lumped single reservoir model with automatically optimised parameters. However, in the present case this fit has been achieved without optimisation in the uncalibrated simulation runs and with a more physically based and spatially distributed model which recognises the spatial heterogeneity in pipe geometry and sources of discharge.

The results corroborate the dominance of the presumed sources of pipeflow in the conceptual model, namely lateral drainage through the pipe walls and bed and a mixture of inputs passing through the mid-slope bogs. The model ignores possible contributions from rainwater infiltrating directly into pipes through the roof and it ignores the capture of overland flow through cracks and blow-holes along the length of the pipe. Both of these seem to be minor sources. Field observations suggest that most overland flow captured by blow-holes is really recycled pipeflow, which has emerged from pipes at points upslope where pipe capacity has been exceeded.

There are a number of empirical simplifications in the model that could be improved upon given more field data. The wetness of the basin at the start of a storm is critical to pipeflow response and a continuous simulation model is likely to produce better estimates of soil water status. Similarly, the method of estimating the movement of the phreatic surface is very empirical and the actual equations are basin specific. But improvements here seem to require a good model of macropore flow and good field data on the nature and distribution of macropores. Darcian models may reasonably be applied, as in this model, to effluent seepage in the pipe horizon. However, the strong evidence for rapid infiltration via fissures in the peaty surface horizons presented, for example, by Sklash et al. (1996) and

Jones and Crane (1984), and the low infiltration rates measured by standard infiltrometry suggest that flow at least within the surface horizon is predominantly non-Darcian.

Perhaps the most immediate of improvements that could be made is in the representation of the pipe network itself. At present, the model represents a tributary pipe as an extra large segment of the main pipe. This has consequences for flow routing and could well contribute to some of the timing errors in the simulations.

4. Conclusions

This is the first attempt to develop a physically realistic, semi-distributed model of pipeflow based on field observations of natural pipes. A number of simplifications have inevitably been made and the exercise has shown the complexity of real-world hill-slope drainage processes. Although the model produced by Nieber and Warner (1991) has an attractive theoretical rigour, it does not attempt to cope with many of the complex sources of pipeflow modelled here, including multiple sources of flow, ephemeral and perennial pipe reaches and a branching network. None of the other models cited are yet as physically based and applicable, albeit in a limited range of conditions, as Nieber and Warner's.

The present model replicates the real field situation well, although the data requirements are substantial and, even so, key parameters such as hydraulic gradients, pipe geometry and network form have been simplified considerably.

The high degree of variability in pipe networks from one basin to another means that the present model requires both detailed surveys of the networks and some hydrological monitoring, for example, of flows and phreatic levels, before it can be applied to a different catchment. Nevertheless, the model clearly represents a step forward in understanding the processes.

Acknowledgements

References

Anderson, M.G., Burt, T.P., 1990. Subsurface run-off. In: Anderson, M.G., Burt, T.P. (Eds.). Process Studies in Hillslope Hydrology. Wiley, Chichester, pp. 365–400.

Barcelo, M.D., Nieber, J.L., 1981. Simulation of the hydrology of natural pipes in a soil profile. American Society of Agricultural Engineers Paper No. 82-2026, St Joseph, MI, 23pp.

Barcelo, M.D., Nieber J.L., 1982. Influence of a soil pipe network on catchment hydrology. American Society of Agricultural Engineers Paper No. 82-2027, St Joseph, MI, 27pp.

Boorman, D.B., Hollis, J.M., Lilly, A., 1995. Hydrology of soil types: a hydrologically based classification of the soils of the United Kingdom. Institute of Hydrology Report No. 126, Wallingford, 137pp.

Bryan, R.B., Harvey, L.E., 1985. Observations on the geomorphic significance of tunnel erosion in a semiarid ephemeral drainage system. Geographis. Ann., Series A 67, 257–273.

Bryan, R.B., Jones, J.A.A., 1997. The significance of soil piping processes: inventory and prospect. Geomorphology 20 (3–4), 209–218.

Burt, T.P., 1992. The hydrology of headwater catchments. In: Calow, P., Petts, G.E. (Eds.). The River Handbook, vol. 1. Blackwell, Oxford, pp. 3–28.

Burt, T.P., Heathwaite, A.L., Labadz, J.C., 1990. Runoff production in peat-covered catchment. In: Anderson, M.G., Burt, T.P. (Eds.). Process Studies in Hillslope Hydrology. Wiley, Chichester, pp. 463–500.

Carey, S.K., Woo, M.-K., 2000. The role of soil pipes as a slope runoff mechanism, Subarctic Yukon. Can. J. Hydrol. 233, 206–222.

Chapman, P.J., 1994. Hydrochemical processes influencing episodic stream water chemistry in a small headwater catchment, Plynlimon, Mid-Wales. Unpublished PhD Thesis, University of London, 416pp.

Chapman, P.J., Reynolds, B., Wheater, H.S., 1993. Hydrochemical change along stormflow pathways in a small moorland headwater catchment in Mid-Wales, U.K. J. Hydrol. 151, 241–265.

Chapman, P.J., Reynolds, B., Wheater, H.S., 1997. Sources and controls of calcium and magnesium in storm runoff: the role of groundwater and ion exchange reactions along water pathways. Hydrol. Earth Syst. Sci. 1 (3), 671–685.

Conacher, A.J., Dalrymple, J.B., 1977. The nine unit land surface

model: an approach to pedogeomorphic research. Geoderma 18 (1/2), 1–154.

Connelly, L.J., 1993. Modelling stormflow in natural subsurface pipes. Unpublished PhD Thesis, University of Wales, Aberystwyth, UK, 419pp.

Dunne, T., 1978. Field studies of hillslope processes. In: Kirkby, M.J. (Ed.). Hillslope Hydrology. Wiley, Chichester, pp. 227–294.

Gardiner, A.T., 1983. Runoff and erosional processes in a peat-moorland catchment. Unpublished MPhil Thesis, Huddersfield Polytechnic, Huddersfield, UK.

Gilman, K., Newson, M.D., 1980. Soil pipes and pipeflow—a hydrological study in upland Wales. Geobooks, Norwich 114pp.

Holden, C., Burt, T.P., 2002. Piping and pipeflow in a deep peat catchment. Catena in press.

Jones, J.A.A., 1971. Soil piping and stream channel initiation. Water Resour. Res. 7 (3), 602–610.

Jones, J.A.A., 1978. Soil pipe networks—distribution and discharge. Cambria 5, 1–21.

Jones, J.A.A., 1981. The nature of soil piping: a review of research. British Geomorphological Research Group, Research Monograph 3. GeoBooks, Norwich 301pp.

Jones, J.A.A., 1987. The effects of soil piping on contributing areas and erosion patterns. Earth Surf. Proc. Landf. 12 (3), 229–248.

Jones, J.A.A., 1988. Modelling pipeflow contributions to stream runoff. Hydrol. Proc. 2, 1–17.

Jones, J.A.A., 1990. Piping effects in humid lands. Groundwater Geomorphology: the Role of Subsurface Water in Earth-Surface Processes and Landforms, Higgins, C.G., Coates, D.R. (Eds.). Geological Society of America, Boulder, Special Paper vol. 252, 111–138.

Jones, J.A.A., 1994. Soil piping and its hydrogeomorphic function. Cuatern. y Geomorfol. 8 (3–4), 77–102.

Jones, J.A.A., 1997a. Pipeflow contributing areas and runoff response. Hydrol. Proc. 11 (1), 35–42.

Jones, J.A.A., 1997b. Subsurface flow and subsurface erosion: further evidence on forms and controls. In: Stoddart, D.R. (Ed.). Process and Form in Geomorphology. Routledge, London, pp. 74–120.

Jones, J.A.A., 1997c. The role of natural pipeflow in dynamic contributing areas and hillslope erosion: extrapolating from the Maesnant data. Phys. Chem. Earth 22 (3–4), 303–308.

Jones, J.A.A., 1997d. Maesnant, Pumlumon (Plynlimon), Wales. In: Gregory, K.J. (Ed.). Fluvial Geomorphology of Great Britain. Joint Nature Conservation Committee Geological Conservation Review Series Chapman and Hall, London, pp. 164–167.

Jones, J.A.A., Crane, F.G., 1984. Pipeflow and pipe erosion in the Maesnant experimental catchment. In: Burt, T.P., Walling, D.E. (Eds.). Catchment Experiments in Fluvial Geomorphology. GeoBooks, Norwich, pp. 55–72.

Jones, J.A.A., Lawton, M., Wareing, D.P., Crane, F.G., 1984. An economical data logging system for field experiments. British Geomorphological Research Group, Technical Bulletin, 31, GeoAbstracts, Norwich, 32 pp.

Jones, J.A.A., Wathern, P., Connelly, L.J., Richardson, J.M., 1991. Modelling flow in natural soil pipes and its impact on plant ecology in mountain wetlands. Nachtnebel, P. (Ed.). Int. Assoc. Hydrol. Sci. Publ. 202, 131–142.

Jones, J.A.A., Richardson, J.M., Jacob, H., 1997. Factors controlling the distribution of piping in Britain: a reconnaissance survey. Geomorphology 20 (3–4), 289–306.

Kirkby, M.J., 1985. Hillslope hydrology. In: Anderson, M.G., Burt, T.P. (Eds.). Hydrological Forecasting. Wiley, Chichester, pp. 37–75.

Kirkham, D., 1949. Flow of ponded water into drain tubes in soil overlying an impervious layer. Trans. Amer. Geophys. Union 30, 369–385.

McCaig, M., 1983. Contributions to storm quickflow in a small headwater catchment: the role of natural pipes and soil macropores. Earth Surf. Proc. Landf. 8 (3), 239–252.

McCaig, M., 1984. The pattern of wash erosion around an upland streamhead. In: Burt, T.P., Walling, D.E. (Eds.). Catchment Experiments in Fluvial Geomorphology. GeoBooks, Norwich, pp. 87–114.

Nieber, J.L., Warner, G.S., 1991. Soil pipe contribution to steady subsurface stormflow. Hydrol. Proc. 5, 345–360.

Putty, M.R.Y., Prasad, R., 2000. Runoff processes in headwater catchments—an experimental study in Western Ghats, South India. J. Hydrol. 235, 63–71.

Roberge, J., Plamondon, A.P., 1987. Snowmelt runoff pathways in a boreal forest hillslope, the role of pipe throughflow. J. Hydrol. 95, 39–54.

Sidle, R.C., Kitahara, H., Terajima, T., Nakai, Y., 1995. Experimental studies on the effects of pipeflow on throughflow partitioning. J. Hydrol. 165 (1–4), 207–219.

Sklash, M.G., Beven, K.J., Gilman, K., Darling, W.G., 1996. Isotope studies of pipeflow at Plynlimon, Wales. Hydrol. Proc. 10 (7), 921–944.

Stagg, M.J., 1974. Rill patterns derived from air photographs of the Gwyne Fach catchment, Black Mountains. Cambria 5 (1), 22–36.

Tanaka, T., 1982. The role of subsurface water exfiltration in soil erosion processes. Int. Assoc. Sci. Hydrol. Publ. 137, 73–80.

Terajima, T., Kitahara, H., Sakamoto, T., Nakai, Y., Kitamura, K., 1996. Pipe flow significance on subsurface discharge from the valley head of a small watershed. J. Jpn For. Soc. 78, 20–28 English abstract.

Terajima, T., Sakamoto, T., Nakai, Y., Kitamura, K., 1997. Suspended sediment discharge in subsurface flow from the head hollow of a small forested watershed, Northern Japan. Earth Surf. Proc. Landf. 22, 987–1000.

Terajima, T., Sakamoto, T., Shirai, T., 2000. Morphology and flow state in soil pipes developed in forested hillslopes underlain by a quaternary sand–gravel formation. Hydrol. Proc. 14, 713–726.

Tsukamoto, Y., Ohta, T., Nogushi, H., 1982. Hydrological and geomorphological studies of debris slides on forested hillslopes in Japan. Int. Assoc. Hydrol. Sci. Publ. 137, 89–98.

Uchida, T., Kosugi, K., Mizuyama, T., 1999. Runoff characteristics of pipeflow and effects of pipeflow on rainfall-runoff phenomena in a mountainous watershed. J. Hydrol. 222 (1–4), 18–36.

Walsh, R.P.D., Howells, K.A., 1988. Soil pipes and their role in runoff generation and chemical denudation in a humid tropical catchment in Dominica. Earth Surf. Proc. Landf. 13 (1), 176–202.

Ward, A.J., 1966. Pipe/shaft phenomena in Northland. J. Hydrol. (New Zealand) 5 (2), 64–72.

Wilson, C.M., Smart, P., 1984. Pipes and pipeflow in an upland catchment. Catena, 11, 145–158.

Woo, M.-K., diCenzo, P., 1988. Pipe flow in James Bay coastal wetlands. Can. J. Earth Sci. 25, 625–629.

Yasuhara, M., 1980. Streamflow generation in a small forested watershed. Unpublished MSc Thesis, University of Tsukuba, 55pp.

Zhu, T.X., 1997. Deep-seated, complex tunnel systems—a hydrological study in a semi-arid catchment, Loess Plateau, China. Piping erosion, Special Issue, Jones, J.A.A., Bryan, R.B. (Eds.). Geomorphology 20, 255–267.

Zhu, T.X., Luk, S.H., Cai, Q.G., 2002. Tunnel erosion and sediment production in the hilly loess region, North China. J. Hydrol. 257 (1–4), 78–90.